



RESEARCH ARTICLE

Visual CRISPR/Cas12a-mediated Rapid Detection of Gyrovirus galga1

Dan Yu^{1,2}, Zhixun Xie^{1,2,*}, Yanfang Zhang^{1,2}, Zhiqin Xie^{1,2}, Sisi Luo^{1,2}, Liji Xie^{1,2}, Meng Li^{1,2}, Qing Fan^{1,2}, Tingting Zeng^{1,2}, Minxiu Zhang^{1,2}, Xiaofeng Li^{1,2}, You Wei^{1,2}, Aiqiong Wu^{1,2} and Lijun Wan^{1,2}

¹GuangXi Key Laboratory of Veterinary Biotechnology, GuangXi Veterinary Research Institute, Nanning 530000, China;

²Key Laboratory of China (GuangXi)-ASEAN Cross-Border Animal Disease Prevention and Control, Ministry of Agriculture and Rural Affairs of China, Nanning 530001, China

*Corresponding author: xiezixun@126.com

ARTICLE HISTORY (25-550)

Received: June 14, 2025
Revised: August 15, 2025
Accepted: August 18, 2025
Published online: February 05, 2026

Key words:

CRISPR/cas12a
Field detection
Gyrovirus galga1
lateral flow strip
Recombinase-aided
amplification
Visual detection

ABSTRACT

The global emergence of gyrovirus galga1 (GyG1) across diverse regions and species underscores the urgent need for rapid diagnostic methods. This study aimed to engineer a field-deployable diagnostic platform for rapid pathogen detection. We established two visual detection methods by integrating recombinase-aided amplification (RAA) and CRISPR/Cas12a technology: RAA–CRISPR/Cas12a combined with fluorescence and RAA–CRISPR/Cas12a combined with lateral flow strips. By systematically optimizing the reaction conditions, the designed primers and crRNA enabled target recognition within 1 hour, and the system exhibited no cross-reactivity with other relevant avian pathogens. RAA–CRISPR/Cas12a combined with fluorescence achieved a detection limit of 2 copies/μL (10 copies/μL visually under UV), and RAA–CRISPR/Cas12a combined with lateral flow strips exhibited a detection limit of 5×10^2 copies/μL. Clinical validation using 192 samples revealed ~10% positivity rates across both novel methods and fluorescence quantitative PCR, with high concordance in positive identification. The results suggest that the two RAA–CRISPR/Cas12a-based visual detection methods established in this study are highly efficient, specific and sensitive and can be used for rapid field detection of GyG1, providing a cost-effective and powerful diagnostic tool for field workers.

To Cite This Article: Yu D, Xie Z, Zhang Y, Xie Z, Luo S, Xie L, Li M, Fan Q, Zeng T, Zhang M, Li X, Wei Y, Wu A and Wan L 2026. Visual CRISPR/Cas12a-mediated rapid detection of gyrovirus galga1. Pak Vet J, 46(2): 438-445. <http://dx.doi.org/10.29261/pakvetj/2026.032>

INTRODUCTION

GyG1, a 2.4 kb ssDNA virus (Anelloviridae family), was first identified in Brazilian chickens in 2011 (Rijsewijk *et al.*, 2011; Varsani *et al.*, 2021). Initially named AGV2 due to its similarity to chicken anemia virus (CAV), it was later recognized as identical to human gyrovirus (HGyV) (>92% nucleotide identity) (Chu *et al.*, 2012; Sauvage *et al.*, 2011). Currently, 15 gyrovirus species exist, classified by VP1 sequence identity (≥69%) (Siddell *et al.*, 2020; Yan *et al.*, 2024). The original AGV2 was officially renamed GyG1 by the International Committee on Taxonomy of Viruses (ICTV) (Varsani *et al.*, 2021).

GyG1 shows global distribution across Asia (China, Japan, Vietnam), Europe (France, Netherlands, Hungary, Italy), South America (Brazil), and Africa (South Africa), primarily infecting chickens but also detected in wild birds, humans, cats, dogs, ferrets, and zoo animals (Biagini *et al.*, 2013; Chu *et al.*, 2012; Feher *et al.*, 2014; Ji *et al.*, 2022), indicating cross-host transmission potential (Liu *et al.*,

2022; Zhang *et al.*, 2024). Regional prevalence varies significantly, from 60.4-90.7% in Brazilian poultry to 1.2-32.1% in Chinese flocks (Dos *et al.*, 2012; Yao *et al.*, 2016; Zhang *et al.*, 2024), with human and ferret infections predominating in Africa and Europe (Biagini *et al.*, 2013; Feher *et al.*, 2014). Coinfections occur in 82% of chicken cases, causing hemorrhagic lesions and systemic inflammation that led to substantial economic losses, compounded by the lack of available vaccines or treatments (Abolnik and Wandrag, 2014; Yao *et al.*, 2017).

The current diagnostic challenges for GyG1 stem from the absence of in vitro culture systems for viral isolation and standardized immunological assays. PCR-based detection remains the primary diagnostic tool but faces limitations: thermal cycling requirements, nonspecific amplification, and limited throughput. Recombinase-aided amplification (RAA) is an emerging isothermal nucleic acid amplification technology, enabling rapid target amplification (30 min) at constant temperatures (37°C ~ 42°C) without thermal cyclers (Tan *et al.*, 2022). The target

specificity and nuclease cleavage activity of clustered regularly interspaced short palindromic repeats (CRISPR) and CRISPR-associated protein (Cas) systems allow CRISPR/Cas technology to achieve ultra-sensitivity and single-nucleotide specificity (Gootenberg *et al.*, 2018). Based on GyG1's dsDNA genome characteristics, we engineered an optimized RAA-CRISPR/Cas12a diagnostic system incorporating dual detection modalities: real-time fluorescence (RAA-CRISPR/Cas12a-FQ) and lateral flow immunoassay (RAA-CRISPR/Cas12a-LFS).

MATERIALS AND METHODS

Samples: The 4 GyG1 strains tested were GX-202307-G1 (GenBank ID: OR921081), GX-202308-B (GenBank ID: PV165310), GX-202403-t8 (GenBank ID: PV165317) and GX-202408-24 (GenBank ID: PV165321). The DNA from 13 related pathogens, including gyrovirus homsa1 (GyH1), chicken infectious anemia virus (CIAV), fowl adenovirus 4 (FAAdV4), H9 subtype avian influenza virus (H9-AIV), Newcastle disease virus (NDV), avian infectious bronchitis virus (IBV), infectious bursal disease virus (IBDV), chicken parvovirus (ChPV), avian leukosis virus (ALV), chicken astrovirus (CAstV), avian nephritis virus (ANV), *Mycoplasma gallisepticum* (MG) and *Mycoplasma synoviae* (MS), were preserved in the laboratory to ensure assay discrimination. Additionally, 192 clinical specimens (120 throat/cloacal swabs; 72 tissue samples) were collected from commercial chicken flocks in Guangxi, China, and frozen at -80°C .

Primer and crRNA design: Three candidate crRNAs (Editgene, Guangzhou, China) were designed through analysis of 58 GyG1 clinical isolates (>95% sequence conservation) retrieved from NCBI using MegAlign software. The spacer sequence was determined based on the protospacer adjacent motif (PAM: 5'-TTTN-3'; N = A/C/G) located on the conserved sequence or its complementary strand, with the 20-bp downstream region of PAM requiring 100% conservation in the first 8-nt seed region (Zetsche *et al.*, 2015). Each crRNA comprised a direct repeat sequence (5'-UAAUUUCUACUAAGUGUAGAU-3') and a unique spacer sequence (Chen *et al.*, 2018).

Additionally, three forward and three reverse primers (Sangon Biotech, Shanghai, China) flanking the target region were designed to prevent pairing with crRNA sequences, with primer lengths of 28-32 bp and amplicon sizes of approximately 300 bp. A plasmid-specific primer pair was also included for template quantification. Both FQ-ssDNA and FB-ssDNA reporters were obtained from Editgene Biotech (Guangzhou, China). All sequences are detailed in Table 1.

Genomic DNA extraction and plasmid standard generation: The collected swab and tissue samples were pre-soaked in PBS and mechanically disrupted (either squeezed or ground). The viral supernatant was transferred to a 32-well plate using a prepackaged viral RNA/DNA extraction kit (Biovet Biotech, Tianjin, China). Subsequently, nucleic acids were purified within 18 minutes using an NPA-32P extraction instrument (Bioer Tech, Hangzhou, China), with genomic DNA collected from designated wells.

Table 1: Sequences of primers, crRNAs and ssDNA reporters.

Name	Sequence (5'→3')
GyG1-F	ATCCAAATTGGTATCGGGTCA
GyG1-R	GCATAAATTCTCGGAGGTTAA
GyG1-F1	ACGGACCAGCTCGCCAGAGATCTACGTC
GyG1-F2	CCAGCTCGCCAGAGATCTACGTCGGCTT
GyG1-F3	CAGCTCGCCAGAGATCTACGTCGGCTTC
GyG1-R1	TAGCCTTACCACATAGGAGCCCCGGGTGT
GyG1-R2	CATAGGAGCCCCGGGTGTGGGTTGAAGAT
GyG1-R3	TTACCACATAGGAGCCCCGGGTGTGGGTT
crRNA-1	UAAUUUCUACUAAGUGUAGAUAGCUUCUACCA CAGAGGACGA
crRNA-2	UAAUUUCUACUAAGUGUAGAUAGUAGCGCGG UAGAAGAUCC
crRNA-3	UAAUUUCUACUAAGUGUAGAUAGCGCGCGU UAAGAGGAGG
FQ-ssDNA	FAM-TTATT-BHQ1
FB-ssDNA	FAM-TTTTTTTATTTTTTT-Biotin

Using purified DNA as the template, PCR amplification was performed with GyG1-F/GyG1-R primers and Tks Gflex™ DNA Polymerase (Takara, Dalian, China). The PCR products were verified by 1.2% agarose gel electrophoresis, and target fragments were purified. The DNA was ligated into a TOPO vector (Aidlab Biotech, Beijing, China) and then transformed into *E. coli* DH5 α (Sangon Biotech, Shanghai, China) via heat shock. Positive clones were screened, and the recombinant plasmid was extracted and designated as the plasmid standard TOPO-S1. The copy number was calculated as follows:

$$\text{Copy number} \left(\frac{\text{copies}}{\mu\text{L}} \right) = \frac{6.02 \times 10^{23} \times \text{ng} / \mu\text{L} \times 10^{-9}}{\text{DNA length} \times 660}$$

Primer and crRNA screening: We screened primers and crRNAs according to manufacturer protocols for the RAA kit (ZhuangBo Biotech Co., Ltd., Nanning, China) and LbCas12a Nuclease (Editgene, Guangzhou, China). The amplification premix was prepared by combining lyophilized enzyme pellets with 25 μL of Buffer A, 13.5 μL of RNase-free water and 2 μL each of the forward and reverse primers (10 μM) in a reaction tube. After adding 5 μL of template DNA to the tube base and 2.5 μL of Buffer B to the cap, the 50 μL reaction system was subjected to three rapid inversions followed by brief centrifugation. Amplification was allowed to proceed at 39 $^{\circ}\text{C}$ for 30 min in a metal-block thermal cycler.

The cleavage mixture contained 3 μL of 10 \times cleavage buffer, 3 μL of LbCas12a nuclease (1 μM), 2 μL of crRNA (500nM), 6 μL of FQ-ssDNA reporter (2 μM) and 15 μL of RNase-free water and was preincubated at room temperature for 15 min. Subsequently, 3 μL of the RAA amplicon was transferred to the cap-containing reaction vessel, followed by immediate vortex mixing, centrifugation, and real-time fluorescence monitoring at 37 $^{\circ}\text{C}$ using a QuantStudio5 qPCR instrument (Thermo Fisher, Massachusetts, USA). The fluorescence intensity was recorded every 30 s for 20 min to quantify cleavage activity.

Optimization of the RAA-CRISPR/Cas12a reaction: Using the standard RAA-CRISPR/Cas12a framework with the plasmid standard TOPO-S1 (positive control) and RNase-free water (negative control), we systematically refined the reaction parameters through fluorescence-based kinetic analysis. A range of

temperatures (37°C, 38°C, 39°C, 40°C, 41°C and 42°C) was methodically evaluated for both amplification and cleavage steps to establish optimal thermal conditions. The concentrations of the primers (200nM, 300nM, 400nM, 500nM and 600nM), crRNA (8.3nM, 16.7nM, 25nM, 33nM, 41.3nM, 50nM and 58nM), based on the assumption that the concentration of the LbCas12a nuclease in the standard system is 33nM) and FQ-ssDNA reporter (200nM, 300nM, 400nM, 500nM and 600nM) were sequentially optimized. The final validation employed FB-ssDNA reporter (50nM, 100nM, 200nM, 300nM, 400nM and 500nM) cross-validated via CRISPR lateral flow strips (Tolo Biotech, Shanghai, China), with optimal concentrations determined by fluorescence and test/control (T/C) line intensity.

Sensitivity and specificity evaluation: To assess the sensitivity of the RAA-CRISPR/Cas12a system, positive plasmids at concentrations spanning seven orders of magnitude (2, 5, 10, 20, 50, 500, and 5000 copies/ μ L) were analyzed via the RAA-CRISPR/Cas12a-FQ method, and real-time fluorescence data and UV-visualized reaction products were recorded. The RAA-CRISPR/Cas12a-LFS method, which was tested across a continuous plasmid gradient ($5.0 \times 10^0 \sim 5.0 \times 10^8$ copies/ μ L), achieved a sensitivity threshold validated by the lateral flow strip T/C line intensity.

Specificity evaluation included screening 13 avian pathogens (GyH1, CIAV, FAdV4, H9-AIV, NDV, IBV, IBDV, ChPV, ALV, ANV, CAstV, MG, MS) with symptoms like GyG1-associated symptoms or those of coprevalent infections. The results were validated by real-time fluorescence curves, UV-induced product fluorescence, and lateral flow strip T/C line readouts.

Practical application in clinical samples: The RAA-CRISPR/Cas12a-FQ and RAA-CRISPR/Cas12a-LFS

methods established in this study were used to analyze 192 clinical samples collected in the laboratory. The results were compared with those of a qPCR assay (Yu *et al.*, 2025) to evaluate the consistency of the three detection methods. All the positive amplicons identified by qPCR were subjected to Sanger sequencing verification (Sangon Biotech, Shanghai, China) to exclude false-positive results.

Statistical analyses: Statistical analyses were performed using GraphPad Prism 8.0 (San Diego, CA, USA) and SPSS 26.0 (IBM, USA). The quantitative data are expressed as the means \pm SEMs. A p value < 0.05 was considered indicative of statistical significance.

RESULTS

Study protocol: Fig. 1 illustrates the RAA-CRISPR/Cas12a workflow for GyG1 detection, which enables rapid, equipment-free pathogen screening. Following nucleic acid extraction, the protocol comprises two core phases. The first is isothermal amplification, wherein the RAA reaction at 37°C \sim 42°C for 30 min generates sufficient target DNA for downstream CRISPR activation; then, CRISPR-Cas12a signal amplification occurs, wherein the Cas12a-crRNA complex binds to target DNA via PAM recognition, triggering collateral ssDNA reporter cleavage. This cascade amplifies fluorescence or lateral flow signals, allowing interpretation by naked eye under UV light or via test strips.

Standard RAA and the CRISPR/Cas12a system: A systematic $3 \times 3 \times 3$ screening strategy (testing 3 forward primers \times 3 reverse primers \times 3 crRNAs) was implemented to identify optimal primer-crRNA combinations. This design generated 27 experimental conditions with matched negative controls (n=54 total reactions), all subjected to 40 cycles of real-time CRISPR-Cas12a fluorescence

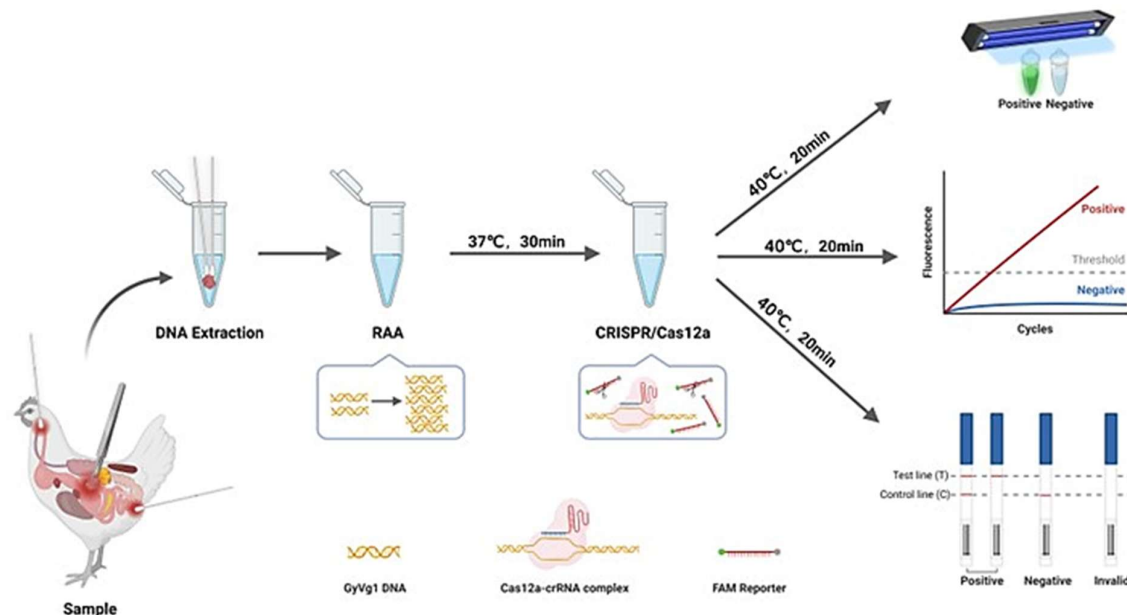


Fig. 1: Process for visual detection of GyG1 via the RAA-CRISPR/Cas12a method. RAA was used for exponential amplification of DNA template. The amplification products were subsequently added to the CRISPR-Cas12a system that can specifically recognize GyG1. Finally, the results can be visualized through an UV light, qPCR instrument or lateral flow strip.

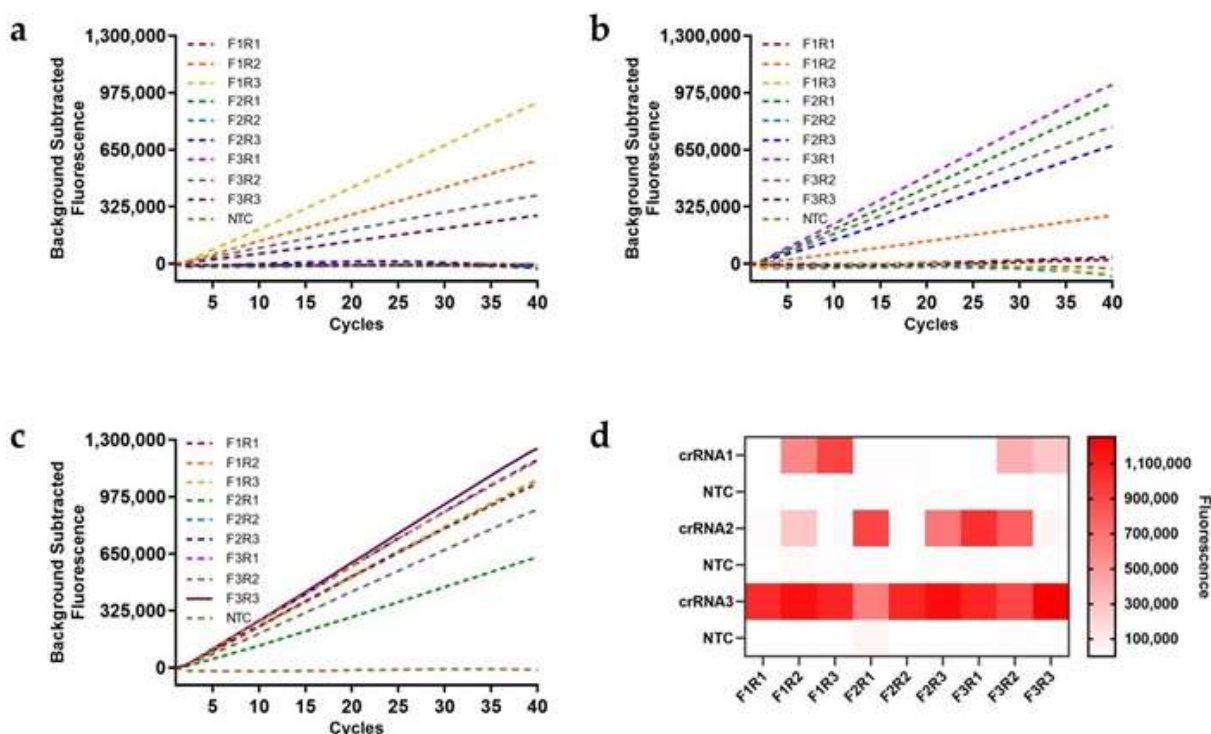


Fig. 2: Process and screening results for visual detection of GyG1 using RAA-CRISPR/Cas12a method. (a) crRNA1 amplification results combined with 9 RAA primer-pairs. (b) crRNA2 amplification results combined with 9 RAA primer-pairs. (c) crRNA3 amplification results combined with 9 RAA primer-pairs. (d) Heatmap of the final fluorescence value at 40 cycles for 54 primer and crRNA combinations.

monitoring. Initial screening showed diminished fluorescence signals with crRNA1 and crRNA2 across all primer sets, evidenced by partial target amplification (Fig. 2a, Fig. 2b). In contrast, crRNA3 consistently produced detectable signals for all primer combinations (Fig. 2c). Critically, the GyG1-F3/GyG1-R3 paired with crRNA3 yielded strong fluorescence in positive samples while showing zero false positives in negative controls (Fig. 2d). These results identify this combination as the optimal detection system.

Ideal reaction conditions for RAA-CRISPR/Cas12a:

Temperature optimization studies identified 37°C as optimal for RAA amplification and 40°C for Cas12a cleavage, yielding peak fluorescence signals and reaction efficiency (Fig. 3a, Fig. 3b). Subsequent component optimization revealed the following: 500 nM primers (Fig. 3c) and 25 nM crRNA (Fig. 3d) achieved 100% target activation, and 500 nM FQ-ssDNA (Fig. 3e) and 300 nM FB-ssDNA (Fig. 3f) maximized the fluorescence and T line intensity. These empirically derived parameters define the optimized RAA-CRISPR/Cas12a system for field diagnostics (summarized in Table 2).

Sensitivity of the RAA-CRISPR/Cas12a assay:

Sensitivity analysis comparing fluorescence (FQ) and lateral flow strip (LFS) readouts revealed distinct detection limits for the RAA-CRISPR/Cas12a platform. As shown in Fig. 4, the fluorescence signal could still be detected when the genomic concentration was 2 copies/ μ L (Fig. 4a), whereas its visual detection limit under UV light reached 10 copies/ μ L (Fig. 4b). Conversely, the lateral flow format demonstrated substantially reduced sensitivity, requiring

5×10^2 copies/ μ L to produce a discernible test-line signal (Fig. 4c). These results highlight the superior analytical performance of fluorescence-based readouts for detection and underscore the practicality of LFS readouts for rapid field applications where moderate sensitivity suffices.

Table 2: Ideal reaction system for RAA-CRISPR/Cas12a

First step: RAA reaction temperature = 37°C		
Component	Volume (μ L)	Concentration
Buffer A	25	
F primer (10 μ M)	2.5	500 nM
R primer (10 μ M)	2.5	500 nM
ddH ₂ O	12.5	
DNA sample	5	
Buffer B	2.5	
Total	50	
Second step: CRISPR/Cas12a reaction temperature = 40°C		
Component	Volume (μ L)	Concentration
10 \times cleavage buffer	3	1 \times
1 μ M LbCas12a nuclease	1	33 nM
250 nM crRNA	3	25 nM
2 μ M FQ-ssDNA reporter (1)	7.5	500 nM
2 μ M FB-ssDNA reporter (2)	4.5	300 nM
ddH ₂ O	8	
RAA product	3	
Total	30	

Specificity of the RAA-CRISPR/Cas12a assay: Both the RAA-CRISPR/Cas12a-FQ and RAA-CRISPR/Cas12a-LFS assays exhibited exceptional specificity in the detection of the GyG1 pathogens, as shown in Fig. 5: the four GyG1 strains triggered corresponding fluorescence (Fig. 5a, Fig. 5b) and distinct T-line signals on test strips (Fig. 5c), whereas all 13 nontarget avian viruses and negative controls exhibited no amplification or nonspecific reactions, confirming zero cross-reactivity across diverse avian pathogens.

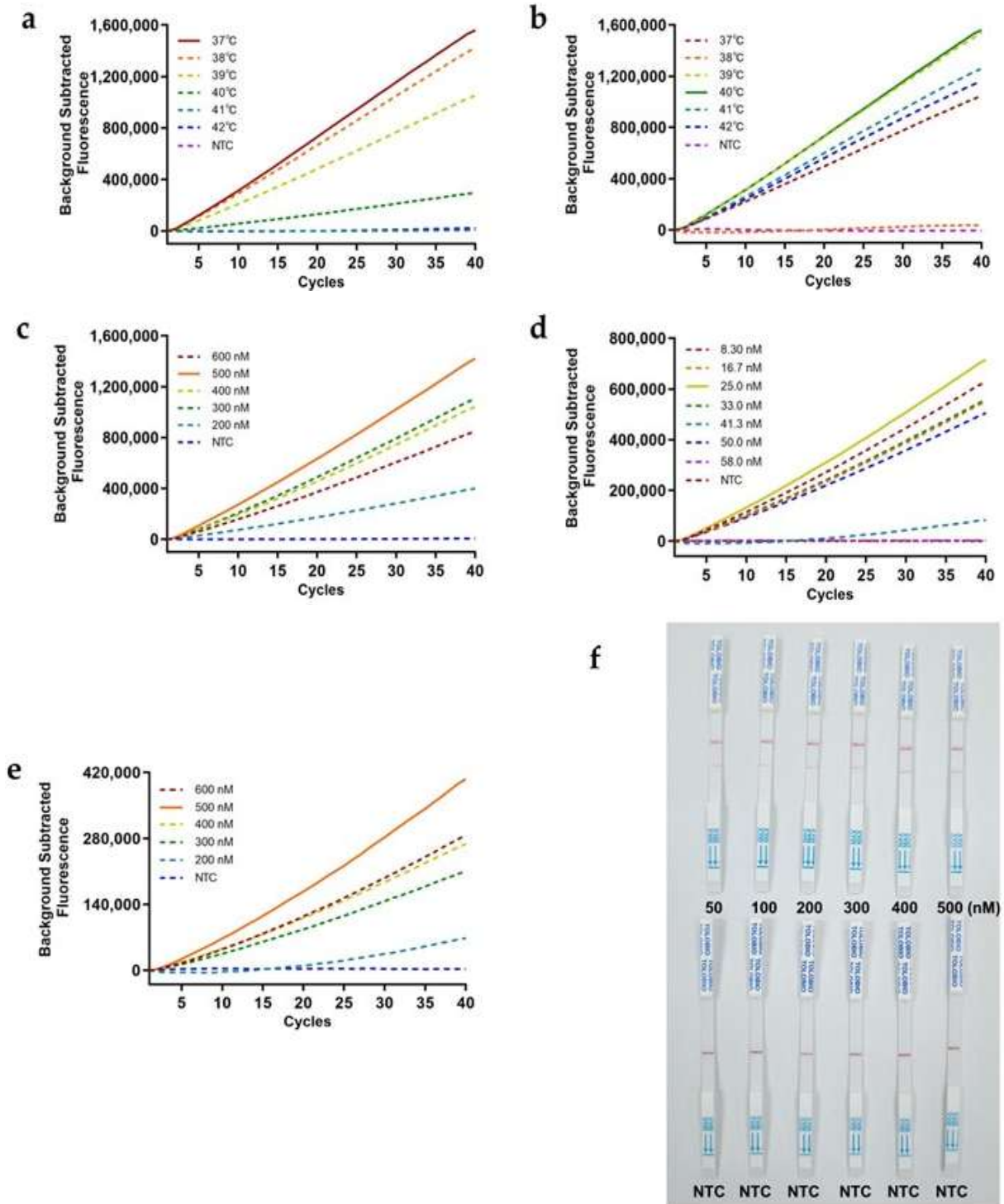


Fig. 3: Results of optimization of the RAA-CRISPR/Cas12a system. **(a)** RAA temperature optimization when the Cas12a cleavage temperature was 40°C. **(b)** Cas12a cleavage temperature optimization when the RAA temperature was 37°C. **(c)** RAA primer concentration. **(d)** crRNA concentration. **(e)** FQ-ssDNA concentration. **(f)** FB-ssDNA concentration.

Practical performance on clinical samples: From 192 clinical samples, qPCR identified 21 positive cases (10.94%, Fig. 6a), a result fully replicated by the fluorescence-based RAA-CRISPR/Cas12a-FQ system (21/192, Fig. 6b). The RAA-CRISPR/Cas12a-LFS assay detected 18 positives (9.38%, Fig. 6c), showing 98.44% (Cohen's $\kappa=0.91$) agreement with the reference method. On the basis of the qPCR standard curve ($Y = -3.321\lg X +$

42.61), the copy numbers of 3 qPCR-positive/LFS-negative samples were calculated as 508 (No.7), 847 (No.10) and 257 (No.13), all of which presented viral loads near the lower limit of detection (LOD) of the LFS assay in real-world samples. This multiplatform evaluation established RAA-CRISPR/Cas12a technology as a robust diagnostic tool with dual-mode adaptability for both laboratory and point-of-care settings.

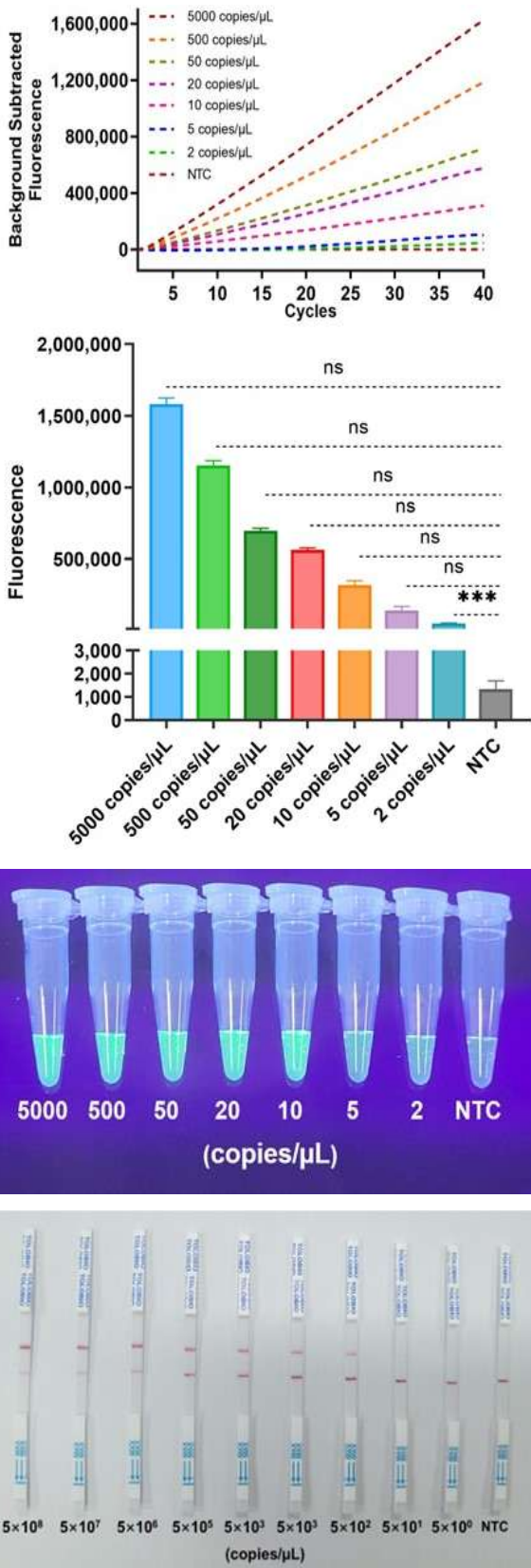


Fig. 4: Sensitivity of the RAA-CRISPR/Cas12a assay. (a) Real-time kinetics for the RAA-CRISPR/Cas12a reactions evoked via the gradient TOPO-SI standard. (b) Results of the final fluorescence value at 40 cycles (n = 3 technical replicates; the results are presented as the means \pm sems; ***, $p < 0.001$). (c) Results of visual observation under UV light. (d) Results of the lateral flow strip assay.

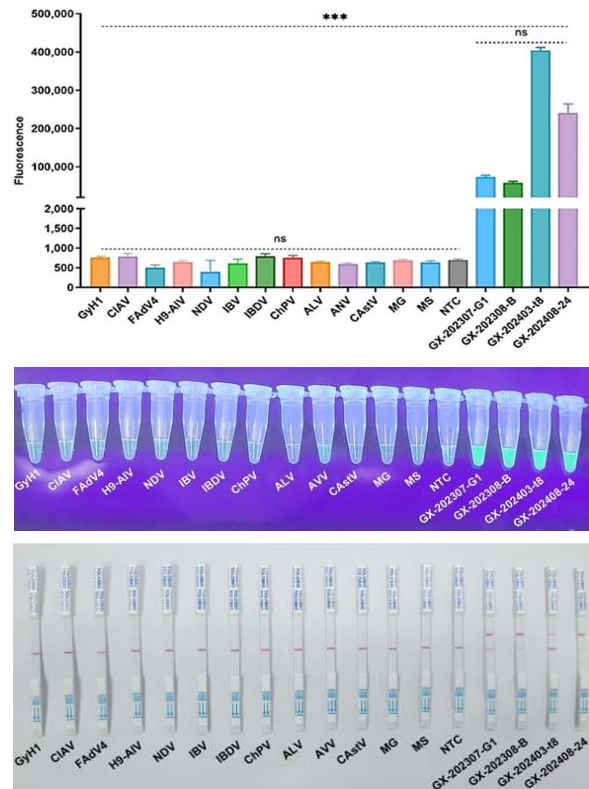


Fig. 5: Specificity of the RAA-CRISPR/Cas12a assay. (a) Results of the final fluorescence value at 40 cycles (n = 3 technical replicates; the results are presented as the means \pm sems; ***, $p < 0.001$). (b) Results of visual observation under UV light. (c) Results of the lateral flow strip assay.

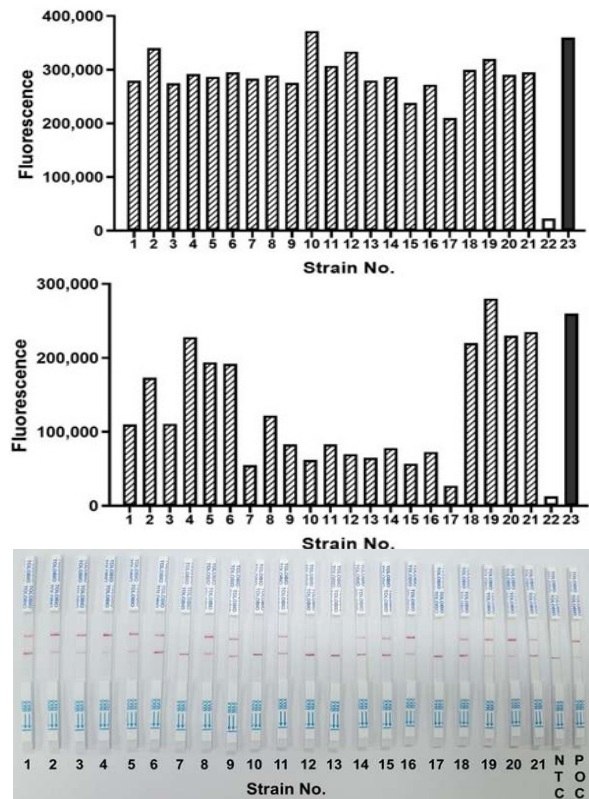


Fig. 6: Comparison of clinical GyGI-positive strains via three assays. (a) Real-time qPCR assay. (b) RAA-CRISPR/Cas12a-FQ assay. (c) RAA-CRISPR/Cas12a-LFS assay.

DISCUSSION

The novel gyrovirus GyG1, with broad zoonotic potential, poses a significant public health threat due to its unique pathogenic dynamics. While GyG1 alone displays limited virulence, its clinical severity emerges through viral synergism, mirroring the high mortality observed in avirulent Newcastle disease virus coinfection (Abolnik and Wandrag, 2014). Alarming, GyG1 contamination has been detected in 28% (9/32) of commercial poultry vaccines (Varela *et al.*, 2014), suggesting that vaccine manufacturing chains constitute a transmission vector contributing to the global dissemination of this virus. Despite its endemic prevalence and worldwide spread, no targeted therapeutics or vaccines have been developed for prevention and control of GyG1 infection, highlighting an urgent unmet need. Given its stealth transmission via subclinical carriers and contaminated biologics, implementing rapid, accurate diagnostic tools for GyG1 identification has become a critical epidemiological need for disrupting transmission cascades and guiding containment strategies.

The advancement of isothermal nucleic acid amplification technologies has transformed pathogen diagnostics, offering practical alternatives to PCR through constant-temperature reactions using simple equipment (Srivastava and Prasad, 2023). Among prevalent techniques (LAMP, RCA, CPA), RAA stands out with its simplified primer design, rapid amplification (<30 min), and moderate thermal requirements—though prone to nonspecific amplification. To overcome this limitation, we developed an integrated RAA-CRISPR/Cas12a platform. This bimodal system combines RAA's target sequence detection with Cas12a's collateral activity for amplicon verification, enhancing both sensitivity and specificity while maintaining field-deployable simplicity—particularly valuable in resource-limited settings.

Through systematic optimization of primer/crRNA selection, temperature, and component concentration, we established a rapid (<1 hour) two-step RAA-CRISPR/Cas12a visual detection platform comprising sequential 30-min isothermal amplification and 20-min Cas12a nonspecific-cleavage phases. This is a deliberate temporal separation strategy that circumvents the sensitivity-compromising risks of premature CRISPR interference in one-pot systems (Xiong *et al.*, 2022; Uno *et al.*, 2023). We developed the RAA-CRISPR/Cas platform for field diagnostics (e.g., farms), where rapid nucleic acid aerosol dissipation enables safe testing. Its temporal separation strategy eliminates premature nonspecific-cleavage by calibrating Cas12a activation via RAA-amplicon thresholds, making this system ideal for on-site applications.

This CRISPR/Cas12a-driven system enables clinic-ready GyG1 diagnosis across settings: fluorescence quantification allows the detection of presymptomatic infections (2 copies/ μL), UV visualization support application in resource-limited laboratories (10 copies/ μL), and the use of LFS strips meet the World Health Organization's ASSURED criteria for field use (5×10^2 copies/ μL), all of which are enabled by VP2-targeted crRNA design, ensuring species specificity. The higher LOD of the LFS method than that of fluorescence-based

detection arises from fundamental differences in detection mechanisms, assay chemistries, and potential inefficiencies in signal generation. While RAA-CRISPR/Cas12a-LFS has 250-fold lower sensitivity than RAA-CRISPR/Cas12a-FQ does, its detection limit aligns with that of real-time fluorescent RAA assays (1×10^2 copies/ μL) (Yu *et al.*, 2024), validating its field applicability. In addition, Our RAA-CRISPR/Cas12a platform balances performance and affordability for field use, with a total cost of ~\$3.50 per test (RAA amplification: \$1.50; CRISPR/Cas12a detection: \$2.00), competitive with LAMP and qPCR (~\$3.00–\$5.00/test). By employing lyophilized RAA pellets and pre-mixed CRISPR reagents, we reduce cold-chain dependence and logistical costs, while the system's minimal equipment needs—a portable heat block (37°C for RAA, 40°C for CRISPR)—eliminate reliance on expensive thermal cyclers or real-time detectors. Further simplifying field deployment, lateral flow strips replace UV lamps or fluorometers for visual readouts. Pilot testing in Guangxi, China, confirmed operational feasibility, where minimally trained personnel successfully implemented the assay using basic water baths, underscoring its suitability for low-resource settings.

The RAA-CRISPR/Cas system achieves high analytical sensitivity, though its two-step workflow may affect reproducibility at low template concentrations (< 10^6 copies/ μL), potentially addressable through real-time RAA quantification or automated liquid handling. Its modular crRNA/primer design enables adaptable GyG1 detection in vaccine batches, though validation in adjuvanted matrices requires further study (Schrader *et al.*, 2012). Building on demonstrated inhibitor tolerance in lyophilized RAA reagents, future optimization should include spike-and-recovery tests with adjuvanted samples to establish robust protocols (Yao *et al.*, 2024).

Conclusions: In conclusion, an RAA-CRISPR/Cas12a detection platform for GyG1 was successfully developed in this study, and two rapid visual detection methods—RAA-CRISPR/Cas12a-FQ and RAA-CRISPR/Cas12a-LFS—were established on the basis of this platform and achieved high sensitivity and specificity. These easy-to-operate and low-cost assays provide powerful point-of-care detection tools for field applications and significantly improve the efficiency of GyG1 diagnosis, endowing the RAA-CRISPR/Cas12a detection platform with broad application prospects.

Authors contribution: writing—original draft preparation, conceptualization, investigation, writing—review and editing, and formal analysis, DY; funding acquisition and project administration, ZX; writing—review and editing, investigation, validation and visualization, YZ; conceptualization, methodology and supervision, ZX; investigation and visualization, QF, SL, LX and ML; formal analysis and validation, TZ, MZ and XL; Data curation, YW, AW and LW. All the authors have read and agreed to the published version of the manuscript.

Funding: This research was funded by the Guangxi Science Base and Talents Special Program, grant number AD17195083; the CARS-Guangxi Poultry Industry Innovation Team, grant number nycytxgxcxtd-2024-19;

Guangxi Key Technologies R&D Program, grant number AB25069499; and the Guangxi BaGui Scholars Program Foundation, grant number 2019A50.

Data availability statement: The original contributions presented in the study are included in the article, and further inquiries can be directed to the corresponding author upon reasonable request.

Acknowledgments: We would like to thank the poultry farmers in various areas and the live poultry market around Guangxi for providing swab and chicken tissue samples and the Key Laboratory of China (Guangxi)-ASEAN Cross-Border Animal Disease Prevention and Control, Ministry of Agriculture and Rural Affairs, Guangxi Key of Veterinary Biotechnology and Guangxi Veterinary Research Institute for providing their support for this study.

Conflicts of interest: The authors declare that they have no conflicts of interest.

REFERENCES

- Abolnik C, Wandrag DB, 2014. Avian gyrovirus 2 and avirulent Newcastle disease virus coinfection in a chicken flock with neurologic symptoms and high mortalities. *Avian Diseases* 58:90-94.
- Biagini P, Bedarida S, Touinssi M, et al., 2013. Human gyrovirus in healthy blood donors, France. *Emerging Infectious Diseases* 19:1014-1015.
- Chu DK, Poon LL, Chiu SS, et al., 2012. Characterization of a novel gyrovirus in human stool and chicken meat. *Journal of Clinical Virology* 55:209-213.
- Dos SH, Knak MB, Castro FL, et al., 2012. Variants of the recently discovered avian gyrovirus 2 are detected in Southern Brazil and The Netherlands. *Veterinary Microbiology* 155:230-236.
- Fehér E, Pazar P, Kovacs E, et al., 2014. Molecular detection and characterization of human gyroviruses identified in the ferret fecal virome. *Archives of Virology* 159:3401-3406.
- Gootenberg JS, Abudayyeh OO, Kellner MJ, et al., 2018. Multiplexed and portable nucleic acid detection platform with Cas13, Cas12a, and Csm6. *Science* 360:439-444.
- Ji J, Yu Z, Cui H, et al., 2022. Molecular characterization of the Gyrovirus galga 1 strain detected in various zoo animals: the first report from China. *Microbes and Infection* 24:104983.
- Liu Y, Lv Q, Li Y, et al., 2022. Cross-species transmission potential of chicken anemia virus and avian gyrovirus 2. *Infection and Genetic Evolution* 99:105249.
- Rijsewijk FA., Dos SH, Teixeira TF, et al., 2011. Discovery of a genome of a distant relative of chicken anemia virus reveals a new member of the genus Gyrovirus. *Archives in Virology* 156:1097-1100.
- Sauvage V, Cheval J, Foulongne V, et al., 2011. Identification of the first human gyrovirus, a virus related to chicken anemia virus. *Journal of Virology* 85:7948-7950.
- Schrader C, Schielke A, Ellerbroek L, et al., 2012. PCR inhibitors - occurrence, properties and removal. *Journal of Applied Microbiology* 113:1014-1026.
- Siddell SG, Walker PJ, Lefkowitz EJ, et al., 2020. Binomial nomenclature for virus species: a consultation. *Archives in Virology* 165:519-525.
- Srivastava P, Prasad D, 2023. Isothermal nucleic acid amplification and its uses in modern diagnostic technologies. *3Biotech* 13:200.
- Tan M, Liao C, Liang L, et al., 2022. Recent advances in recombinase polymerase amplification: Principle, advantages, disadvantages and applications. *Frontiers in Cellular and Infection Microbiology* 12:1019071.
- Uno N, Li Z, Avery L, et al., 2023. CRISPR gel: A one-pot biosensing platform for rapid and sensitive detection of HIV viral RNA. *Analytica Chimica Acta* 1262:341258.
- Varela AP, Dos SH, Cibulski SP, et al., 2014. Chicken anemia virus and avian gyrovirus 2 as contaminants in poultry vaccines. *Biologicals* 42:346-350.
- Varsani A, Opriessnig T, Celer V, et al., 2021. Taxonomic update for mammalian anelloviruses (family Anelloviridae). *Archives in Virology* 166:2943-2953.
- Xiong Y, Cao G, Chen X, et al., 2022. One-pot platform for rapid detecting virus utilizing recombinase polymerase amplification and CRISPR/Cas12a. *Applied Microbiology and Biotechnology* 106:4607-4616.
- Yan TX, Wang Z, Li R, et al., 2024. Gyrovirus: current status and challenge. *Frontiers in Microbiology* 15:1449814.
- Yao S, Gao X, Tuo T, et al., 2017. Novel characteristics of the avian gyrovirus 2 genome. *Scientific Reports* 7:41068.
- Yao S, Tuo T, Gao X, et al., 2016. Avian gyrovirus 2 in poultry, China, 2015-2016. *Emerging Microbes and Infections* 5:e112.
- Yao Z, He K, Wang H, et al., 2024. Tuning the dynamic reaction balance of CRISPR/Cas12a and RPA in one pot: A key to switch nucleic acid quantification. *ACS Sensors* 9:3511-3519.
- Yu D, Xie ZX, Zhao JK, et al., 2025. Establishment of the duplex real-time PCR detection method for gyrovirus galga 1 and gyrovirus homsa 1. *Chinese Journal of Veterinary Science* 45:59-65.
- Yu D, Zhao JK, Yu HY, et al., 2024. Establishment of the real-time RAA detection method for Gyrovirus galga 1. *Chinese Veterinary Science* 54:1577-1585.
- Zhang F, Xie Q, Yang Q, et al., 2024. Prevalence and phylogenetic analysis of Gyrovirus galga 1 in southern China from 2020 to 2022. *Poultry Science* 103:103397.
- Zhang Z, Man Y, Xu X, et al., 2024. Genetic heterogeneity and potential recombination across hosts of Gyrovirus galga 1 in central and eastern China during 2021 to 2024. *Poultry Science* 103:104149.